Journal of Photonics for Energy

SPIEDigitalLibrary.org/jpe

Numerical modeling of silicon evanescent lasers

Alexey G. Rzhanov
Stanislav E. Grigas

SPIE

Numerical modeling of silicon evanescent lasers

Alexey G. Rzhanov and Stanislav E. Grigas
M.V. Lomonosov Moscow State University, Faculty of Physics, Leninskie Gory,
Moscow 119991, Russia
moonlight_14@mail.ru

Abstract. A numerical self-consisted dynamic model of a silicon evanescent laser is presented. This model allows us to calculate the laser output power as a function of drive current and mode composition. Obtained results are in good agreement with published experimental data. Dynamic processes in silicon evanescent lasers are also investigated, and self-modulation processes are observed. *© 2011 Society of Photo-Optical Instrumentation Engineers (SPIE)*. [DOI: 10.1117/1.3523319]

Keywords: silicon lasers; numerical simulations; dynamical models.

Paper 10114SSPR received Jul. 28, 2010; revised manuscript received Sep. 25, 2010; accepted for publication Oct. 15, 2010; published online Jan. 28, 2011.

1 Introduction

Over the past few years silicon photonics has experienced tremendous growth.[1–4] The main reason is compatibility with CMOS technology, which allows one to use existing semiconductor fabrication techniques and provides fabrication of low-cost optoelectronic devices. Significant progress has been made in the fabrication of passive silicon-based devices such as modulators,[5] photodetectors,[6] and interconnects,[7] but still it is difficult to achieve lasing in silicon because of its indirect bandgap. Different approaches to fabricate silicon lasers have been demonstrated, including nanocrystalline silicon structures,[8] Si/Ge quantum cascade structures,[9–11] and Raman lasers,[12] but the resulting efficiencies are very low. For example, the efficiency of a silicon nanocrystal-based LED is 0.1% (Ref. 13) and the efficiency of a Raman silicon laser is 8.5% (Ref. 12). The most successful approach to considerably increase silicon laser efficiency is the hybrid integration of a III–V quantum-well heterostructure with a silicon waveguide.[14–18] This type of laser is called a hybrid silicon evanescent laser (SEL). Thus, differential quantum efficiencies of optical pumped and electrical pumped SELs are 15% (Ref. 19) and 46% (Ref. 15), respectively. A great deal of experimental data can be found in the literature concerning SELs, but there is still a need for theoretical research in this area. A numerical self-consistent dynamic model of electrically pumped hybrid silicon evanescent lasers is presented in this work.

2 Numerical Simulation

A cross section of an electrically pumped SEL is schematically shown in Fig. 1 (Ref. 15). The laser consists of two regions: a silicon-on-insulator (SOI) passive rib waveguide and a InGaAlAs/InP active region that provides optical gain. The SOI waveguide width w is 2.5 μm, height h is 0.69 μm, and rib etch depth d is 0.52 μm. The active region is based on AlGaInAs quantum wells with photoluminescence peaks at 1303 nm. Optical radiation propagates mainly through the silicon waveguide. Laser gain in such a structure is achieved due to the silicon waveguide optical mode overlapping with an active layer.

We have developed a numerical self-consistent dynamic model of the SEL based on these assumptions: quasi-stationary approximation, uniform distribution of light intensity and carrier concentration in the z-y plane, and neglected carrier diffusion.

1947-7988/2011/$25.00 © 2011 SPIE

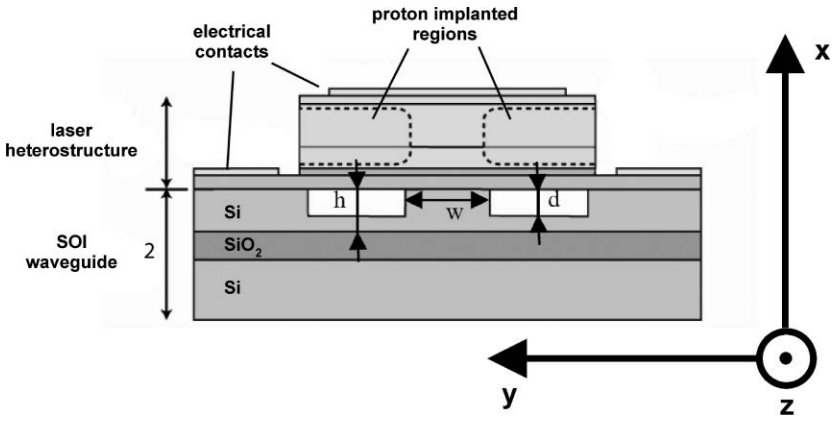

Fig. 1 Silicon evanescent laser structure (Ref. 15).

Carrier concentration and photon density dynamics in the resonator are described by coupled rate equations (for example, see Ref. 20). On the assumptions mentioned above, these equations take on the form

$$\frac{dN(t)}{dt} = \frac{J}{ed} - \frac{N(t)}{\tau_{sp}} - \sum_{i=1}^{m} \tilde{\Gamma}_i G_i(t) S_i(t), \tag{1}$$

$$\frac{dS_1(t)}{dt} = \tilde{\Gamma}_1 \Gamma G_1(t) S_1(t) - \frac{S_1(t)}{\tau_p} + \Gamma\beta \frac{N(t)}{\tau_{sp}}, \tag{2}$$

$$\frac{dS_m(t)}{dt} = \tilde{\Gamma}_m \Gamma G_m(t) S_m(t) - \frac{S_m(t)}{\tau_p} + \Gamma\beta \frac{N(t)}{\tau_{sp}}, \tag{3}$$

where $S_i(t)$ is the resonator volume-averaged i'th optical mode photon density, $N(t)$ is the active layer volume-averaged carrier concentration, J is the pump current density, e is the electron charge, d is the active layer thickness, τ_{sp} is the carrier spontaneous recombination time, τ_p is the photon lifetime in the resonator, β is the spontaneous recombination coefficient (fraction of spontaneous radiation that is amplified), $G_i(t)$ is the i'th mode optical gain, Γ and $\tilde{\Gamma}_i$ are optical confinement factors, and m is the number of transversal optical modes that are taken into account.

The first equation states that the speed of carrier concentration variations depends on spontaneous and stimulated recombination rates and electrical pumping. Second and subsequent equations state that photon density variation speed depends on photon production rate, spontaneous recombination rate, and photon losses in the resonator.

Intensity evolution of the i'th optical mode can be described in terms of gain coefficients $G_i(t)$, which can be calculated as:

$$G_i(t) = -2 \operatorname{Im} \omega_i(t), \tag{4}$$

where Im represents the imaginary part of a complex number.

These gain coefficients are time dependent, because the i'th optical mode complex frequency ω_i (complex eigenvalue of wave equation) varies with time. To obtain $G_i(t)$, resonant frequencies ω_i are calculated in the first stage from resonator parameters by solving a scalar wave equation. Then, gain coefficients are used to calculate carrier concentrations at the next time step from Eqs. (1)–(4). Carrier concentration variations lead to active layer refractive index variation; thus, it is necessary to recalculate resonant frequencies at which laser generation occurs and optical modes gain coefficients at every time step in a finite-difference algorithm. Total computational

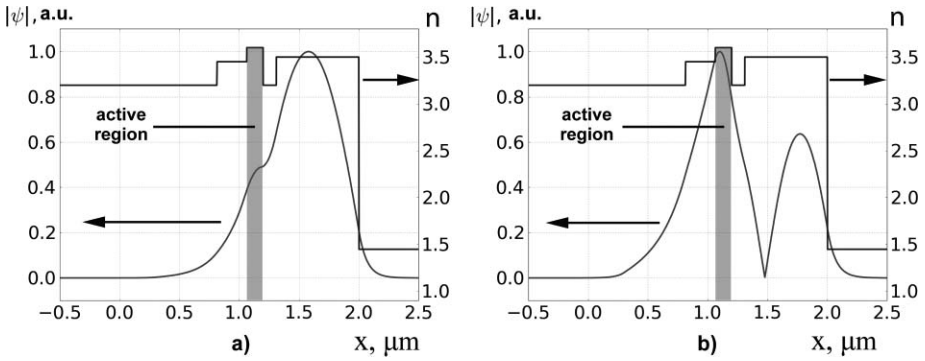

Fig. 2 Hybrid laser structure optical mode profiles: (a) TE_0 and (b) TE_0, where $|\psi|$ is the magnitude of the normalized nonzero electrical field component and n is the profile of the real part of the refractive index.

time directly depends on the time required for resonant frequency calculation. To decrease this time and enhance computational efficiency of the algorithm, we used a special computational technique that was proposed earlier in Ref. 21.

3 Results and Discussion

Two lower order optical mode profiles calculated at the beginning of the simulation are shown in Fig. 2. Spatial intensity distribution was calculated at every time step during the simulation, with resonator optical property variations taken into account. The confinement factor, defined as the ratio of the average value of electromagnetic field intensity in the active region to its average value in the resonator, was calculated for each optical mode:

$$\tilde{\Gamma}_i = \frac{\int_{V_{\text{act}}} |\psi_i(x)|^2 dV / V_{\text{act}}}{\int_{V_{\text{cav}}} |\psi_i(x)|^2 dV / V_{\text{cav}}},$$

where $\psi_i(x)$ is the i'th optical mode profile, V_{act} is the active region volume, and V_{cav} is the cavity volume. Confinement factor Γ is defined as the ration of the active region volume to the volume of the whole resonator: $\Gamma = V_{\text{act}}/V_{\text{cav}}$.

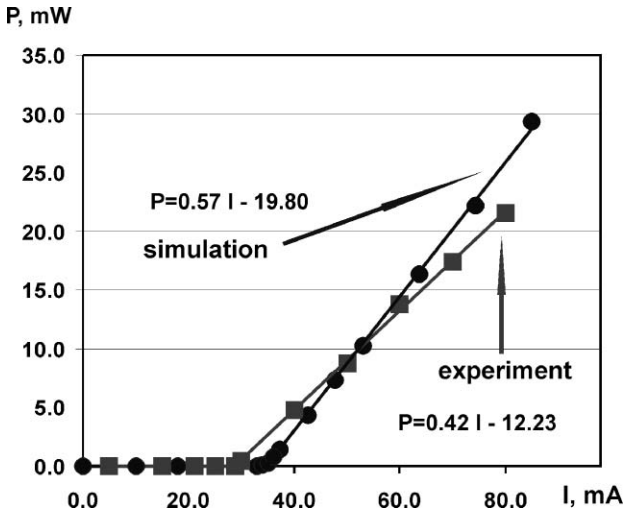

Fig. 3 SEL's output power P as a function of drive current I. Experimental data (Ref. 15) and obtained numerical results are presented.

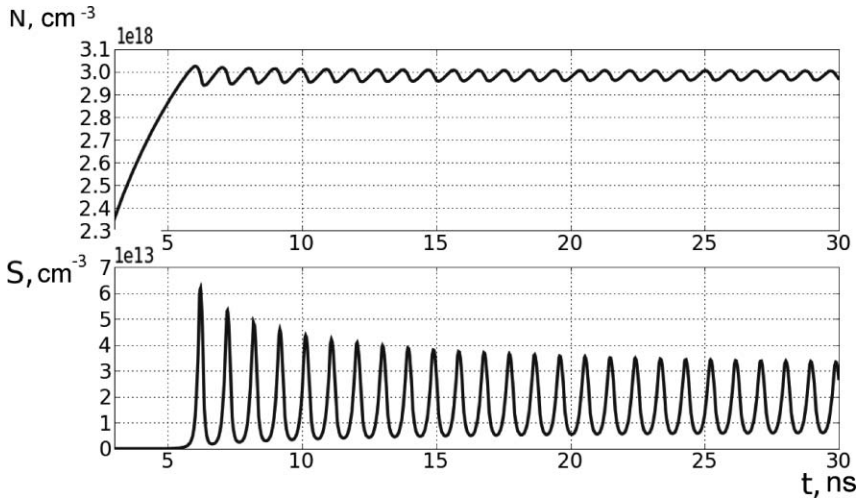

Fig. 4 Self-modulation in an SEL at 1.22 times the threshold pump current, where *N* is the carrier concentration in the active region and *S* is the photon density in the resonator.

The proposed algorithm was used to determine laser structure mode composition. As follows from Fig. 2, the first-order mode overlapping with an active region is considerably higher than that for the fundamental mode. Therefore, laser generation is expected only for the first-order mode. This result is confirmed by experimental data.[15] Thus, spatial separation between the active region and silicon waveguide leads to laser single-mode operation.

Output radiation intensity as a function of time for a given pump current value was calculated. After the transient processes finished, output radiation power could be evaluated. Implementation of this procedure to several pump current values allows us to obtain laser P–I characteristics. These characteristics and corresponding experimental data[15] are shown in Fig. 3. Approximations for linear sections of P–I characteristics are also presented. Calculated values of threshold current and curve slope—31 mA and 0.57 W/A, correspondingly—are in good agreement with experimental data of a threshold pump current of 29 mA and linear section slope of 0.42 W/A.

Dynamic properties of SELs were also investigated. It was shown that the laser current-step response is the typical inversion population and photon density relaxation oscillation process. When the pump current reaches some critical value, the laser response takes the form of periodical self-sustained pulses. An example of such a self-modulation process at 1.22 times the threshold pump current is shown in Fig. 4. The oscillation frequency is ~1 GHz. Self-modulation in SELs is of great interest because it provides a higher signal-to-noise ratio in optical communication and optical storage read-write systems.

4 Conclusion

A self-consisted dynamic model of a silicon evanescent laser based on the numerical solution of a scalar wave equation and coupled rate equations is developed. In order to enhance the computational efficiency of the proposed method, a special technique for resonant frequency calculation from the resonator parameters is utilized.

The SEL's output power as a function of drive current and its mode composition are obtained. These results are in good agreement with published experimental data. The proposed model also allows us to investigate dynamic processes in hybrid lasers. It is shown that the SEL's current-step response is the typical inversion population and photon density relaxation oscillation process. Under certain conditions, periodical self-sustained pulses are observed.

Acknowledgments

The authors thank A. S. Logginov for his support and encouragement.

References

1. B. Jalali, M. Paniccia, and G. Reed, "Silicon photonics." *IEEE Microwave Mag.* **7**, 58–68 (2006).
2. L. Tsybeskov, D. J. Lockwood, and M. Ichikawa, "Silicon photonics: CMOS going optical," *Proc. IEEE* **97**, 1161–1165 (2009).
3. R. A. Soref, "Silicon-based optoelectronics," *Proc. IEEE* **81**, 1687–1706 (1993).
4. O. Bisi, S. U. Campisano, L. Pavesi, and F. Priolo, *Silicon Based Micro-Photonics: From Basics to Applications*, p. 279, IOS Press, Amsterdam (1999).
5. D. Marris-Morini, L. Vivien, G. Rasigade, J.-M. Fedeli, E. Cassan, X. L. Roux, P. Crozat, S. Maine, A. Lupu, P. Lyan, P. Rivallin, M. Halbwax, and S. Laval, "Recent progress in high-speed silicon-based optical modulators," *Proc. IEEE* **97**, 1199–1215 (2009).
6. L. Vivien, J. Osmond, J.-M. Fedeli, D. Marris-Morini, P. Crozat, J.-F. Damlencourt, E. Cassan, Y. Lecunff, and S. Laval, "42 GHz p.i.n. germanium photodetector integrated in a silicon-on-insulator waveguide," *Opt. Express* **17**, 6252–6257 (2009).
7. A. Sure, T. Dillon, J. Murakowski, C. C. Lin, D. Pustai, and D. W. Prather, "Fabrication and characterization of three-dimensional silicon tapers," *Opt. Express* **11**, 3555–3561 (2003).
8. L. T. Canham, "Silicon quantum wire array fabrication by electrochemical and chemical dissolution of wafers," *Appl. Phys. Lett.* **57**, 1046–1048 (1990).
9. R. A. Soref, "Prospects for novel Si-based optoelectronic devices: unipolar and p-i-p-i lasers," *Thin Solid Films* **294**, 325–329 (1997).
10. G. Dehlinger, L. Diehl, U. Gennser, H. Sigg, J. Faist, K. Ensslin, and D. Grutzmacher, "Intersubband electroluminescence from silicon-based quantum cascade structures," *Science* **290**, 2277–2280 (2000).
11. L. Diehl, S. Mentese, H. Sigg, E. Muller, D. Grutzmacher, U. Gennser, I. Sagnes, T. Fromherz, J. Stangl, T. Roch, G. Bauer, Y. Campidelli, O. Kermarrec, D. Bensahel, and J. Faist, "Electroluminescence from strain compensated $Si_{0.2}Ge_{0.8}$/Si quantum-cascade structures based on a bound-to-continuum transition," *Appl. Phys Lett.* **81**, 4700–4702 (2002).
12. O. Boyraz and B. Jalali, "Demonstration of a silicon Raman laser," *Opt. Express* **12**, 5269–5273 (2003).
13. G. Franzò, A. Irrera, E. C. Moreira, M. Miritello, F. Iacona, D. Sanfilippo, G. Di Stefano, P. G. Fallica, and F. Priolo, "Electroluminescence of silicon nanocrystals in MOS structures," *Appl. Phys. A* **74**, 1–5 (2002).
14. H. Park, A. W. Fang, S. Kodama, and J. E. Bowers, "Hybrid silicon evanescent laser fabricated with a silicon waveguide and III–V offset quantum wells," *Opt. Express* **13**, 9460–9464 (2005).
15. H.-H. Chang, A. W. Fang, M. N. Sysak, H. Park, R. Jones, O. Cohen, O. Raday, M. J. Paniccia, and J. E. Bowers, "1310 nm silicon evanescent laser," *Opt. Express* **15**, 11466–11471 (2007).
16. B. R. Koch, A. W. Fang, O. Cohen, and J. E. Bowers, "Mode-locked silicon evanescent lasers," *Opt. Express* **15**, 11225–11233 (2007).
17. A. W. Fang, E. Lively, Y.-H. Kuo, D. Liang, and J. E. Bowers, "A distributed feedback silicon evanescent laser," *Opt. Express* **16**, 4413–4419 (2008).
18. A. W. Fang, M. N. Sysak, B. R. Koch, R. Jones, E. Lively, Y.-H. Kuo, D. Liang, O. Raday, and J. E. Bowers, "Single-wavelength silicon evanescent lasers," *J. Sel. Top. Quant. Electron.* **15**, 535–544 (2009).

19. A. W. Fang, H. Park, S. Kodama, and J. E. Bowers, "An optically pumped silicon evanescent laser," in *31st European Conf. Opt. Commun*., IEE Conf. Pub. 2005, v6-57 (2005).
20. B. Mroziewicz, M. Bugajski, and W. Nakwaski, *Physics of Semiconductor Lasers*, p. 366, PWN, Warszawa (1991).
21. A. G. Rzhanov and S. E. Grigas, "Determination of guided modes in multilayer dielectric waveguides," *Numer. Meth. Program.* **10**, 72–76 (2009).

Alexey G. Rzhanov is an assistant professor at the M.V. Lomonosov Moscow State University, where he received his MS in physics in 1984 and PhD in radio physics and quantum electronics in 1994. He is the author of more than 40 journal papers. His current research interests include injection laser and photovoltaic light converters modeling and photonic and optoelectronic systems.

Stanislav E. Grigas received his MS in physics from the M.V. Lomonosov Moscow State University in 2010, where he is currently a PhD student. He is the author of two journal papers. His current area of research is the modeling and numerical simulation of optoelectronic devices. His main areas of interest include silicon photonics, semiconductor lasers, and optical waveguides.